GEOPHYSICAL RESEARCH LETTERS, VOL. 37, L08104, doi:10.1029/2009GL042117, 2010

Motion of aurorae

Christopher. C. Chaston,[1] Kanako Seki,[2] Takeshi Sakanoi,[3] Kazushi Asamura,[4] and Masafumi Hirahara[5]

Received 10 December 2009; revised 11 February 2010; accepted 8 March 2010; published 21 April 2010.

[1] Using high resolution auroral imagery and particle measurements from the Reimei spacecraft we distinguish 'Alfvénic' and 'quasi-static' auroral forms and implement a new multi-scale wavelet analysis technique to examine how the vorticity in these forms varies as a function of scale transverse to the geomagnetic field. We find from this analysis that the complex motions of aurorae can be described by power-laws relating spatial scale to optical vorticity. We demonstrate how these relationships naturally arise from the 'conductance' of geomagnetic field-lines and the physics of Alfvén waves. **Citation:** Chaston, C. C., K. Seki, T. Sakanoi, K. Asamura, and M. Hirahara (2010), Motion of aurorae, *Geophys. Res. Lett.*, *37*, L08104, doi:10.1029/2009GL042117.

1. Introduction

[2] Spacecraft observations of accelerated electron distributions and electromagnetic fields at high latitudes have allowed the identification of quasi-static potential structures [*Mozer et al.*, 1977; *Ergun et al.*, 1998] and small-scale Alfvén waves [*Stasiewicz et al.*, 2000] as drivers of the discrete aurora. The 'quasi-static' aurora is so called because the transit time of an electron through the accelerating field-aligned potential is small relative to the time-scale for variation of the potential. As a consequence electrons accelerated through these structures are shifted in energy giving rise to what are commonly identified in electron energy-time spectrograms as 'inverted-Vs' [*Frank and Ackerson*, 1972]. However, when the electron transit time approaches the time scale of variation of the accelerating potential structure the manner in which an electron interacts with the fields is complicated through the action of Landau resonance [*Lysak and Lotko*, 1996] and Fermi-like acceleration [*Kletzing*, 1994] processes. These processes acting above the auroral ionosphere lead to flat-top and often time-dispersed electron energy spectra in differential energy flux [*Chaston et al.*, 2003] that are the hallmark of the 'Alfvénic' or wave-like aurora. In both the quasi-static and Alfvénic cases however the time varying electromagnetic fields which provide the Poynting flux to power the acceleration process can be described as Alfvén waves [*Lysak and Dum*, 1983]. In this sense the terms quasi-static and Alfvénic represent opposite limits of the relationship between electron transit-time and the time-scale for variation of auroral electromagnetic fields. These classifications therefore provide a qualitative but nonetheless useful means for distinguishing different acceleration mechanisms in auroral electron energy-time spectrograms.

[3] While the distinction between the quasi-static and Alfvénic aurora from electron measurements is well established, the same distinction from optical observations of the associated auroral forms is not. This is because of the inherent difficulty in obtaining particle and optical measurements that are magnetically conjugate with an accuracy extending to small-scales. Consequently there are few studies [e.g., *Stenbaek-Nielsen et al.*, 1998; *Hallinan et al.*, 2001; *Asamura et al.*, 2009] where correlations between particle measurements and small-scale auroral forms have been performed. In this report we unambiguously distinguish quasi-static and Alfvénic aurora using imager and particle observations from the polar orbiting spacecraft Reimei [*Sakanoi et al.*, 2003; *Asamura et al.*, 2003] that routinely records magnetically conjugate particle and optical measurements down to kilometre scales. We demonstrate how the multi-scale motions of the auroral forms associated with the quasi-static and Alfvénic aurora differ and show how these motions are consistent with a quasi-static and Alfvénic description of electromagnetic fields along an auroral field-line.

2. Observations

[4] Figure 1 shows a schematic of recent observations performed by the Reimei spacecraft [*Obuchi et al.*, 2008]. The auroral imagery snapshots shown in this figure at times t_1 and t_2 correspond to Alfvénic and quasi-static aurora respectively. This light was recorded at ~670 nm due to prompt emission from N_2 which allows us to resolve the rapid motions which are the subject of this report. The identification as Alfvénic or quasi-static is based on simultaneous measurements of energetic Earthward streaming electrons on the same geomagnetic field-lines from Reimei at an altitude of 650 km as shown in Figure 2a. These measurements reveal electrons broadly distributed and somewhat time-dispersed in energy from 09:31:40–09:31:50 UT indicative of the Alfvénic aurora and those more closely distributed around a single energy from 09:31:50–09:32:00 UT at >10 keV indicative of the quasi-static aurora in the form of an 'inverted-V'. Expanded views of the auroral snapshots for the Alfvénic and quasi-static aurora are shown in Figures 2b and 2c respectively. The exact foot-point of the magnetic field connecting the upper

[1]Space Sciences Laboratory, University of California, Berkeley, California, USA.
[2]Solar Terrestrial Environment Laboratory, University of Nagoya, Nagoya, Japan.
[3]Graduate School of Science, Planetary Plasma and Atmospheric Research Centre, University of Tohoku, Sendai, Japan.
[4]Institute of Space and Astronautical Science, Japan Aerospace Exploration Agency, Kanagawa, Japan.
[5]Department of Earth and Planetary Science, Graduate School of Science, University of Tokyo, Tokyo, Japan.

0094-8276/10/2009GL042117

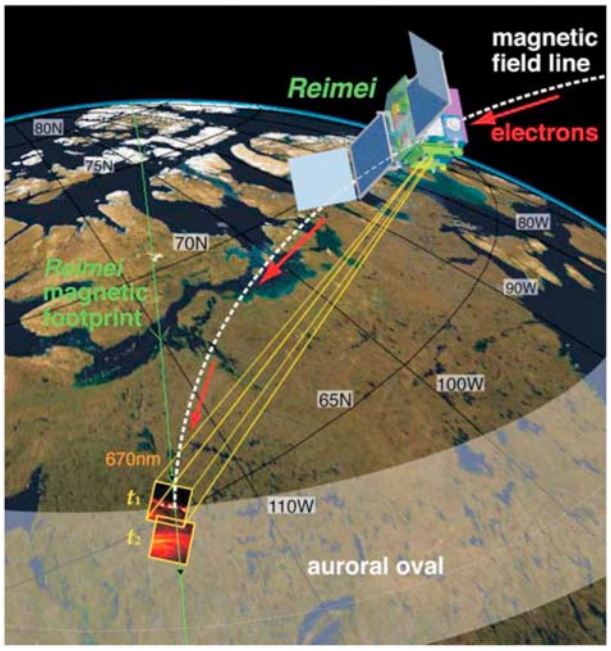

Figure 1. Schematic view of the Reimei spacecraft simultaneously measuring auroral imagery and electrons streaming Earthward along the geomagnetic field. The white shaded area shows the location of the auroral oval where aurora are most commonly observed. The white dashed line is the geomagnetic field and the green line is the track of the Reimei spacecraft projected to an altitude of 105 km along the geomagnetic field. The thumbnail images at t_1 and t_2 show snapshots of the Alfvénic and Quasi-static aurora respectively at 670 nm. Here t_1 = 2005-12-22/09:31:45.9 and t_2 = 2005-12-22/09:31:53.4 UT.

atmosphere at 105 km altitude to the electrons observed at the spacecraft are shown by the X's in each image along with the corresponding time. These images show that the aurora associated with each acceleration process have some differences in form, however it is the variation in motion of these forms as a function of scale which provide the most cogent insights into the acceleration processes which drive them.

[5] To quantitatively examine the motion of auroral features as a function of scale in a sequence of images from the Reimei spacecraft we implement a new technique based on 2-D wavelet transforms. We reserve a detailed description of this approach for another forum but here provide a sketch of how it works. For complex basis functions the technique provides a measure of the amplitude of the intensity and phase as a function of scale and position in the camera field of view. For images interpolated onto the same spatial grid the phase difference between consecutive images at the same location corresponds to a spatial shift defined as $(\Delta\varphi/2\pi)\lambda_F$ where λ_F is the corresponding Fourier wavelength or scale for the wavelet used. Since the time between images is known, a velocity vector can therefore be derived at each location and scale within the camera field of view. To perform the analysis we use Paul wavelets [*Torrence and Compo*, 1998] which provide good spatial localisation without sacrificing scale resolution when applied to the spatial derivative of the luminosity. The small arrows in Figures 2b–2e show results of the application of this procedure to consecutive images of the Alfvénic and quasi-static aurora. These results are derived at a scale perpendicular to the geomagnetic field of 5 km at an emission altitude of 105 km. We have performed tests to confirm the reliability of this technique both through application to synthetic imagery data and by comparison to traditional correlation approaches [*Ebihara et al.*, 2007]. In the present case, the white contours show the 90% confidence level above noise for the velocity determination. The vectors within these contours are reliable velocity measurements plotted at half resolution and reveal rotation and shears in the optical features at this scale.

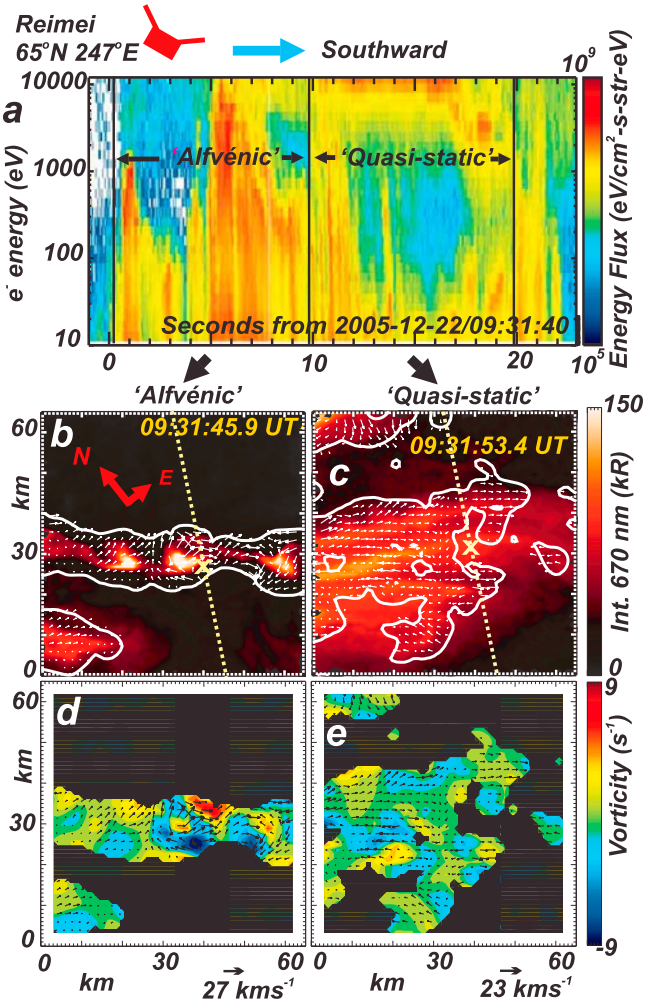

Figure 2. Auroral electron and camera observations. (a) Electron energy spectrogram showing the electron energy fluxes responsible for the auroral emission at 670 nm shown for the (b) Alfvénic and (c) Quasi-static aurora and in Figure 1 at t_1 and t_2. Small arrows show the flow velocity at half resolution of the optical features at a scale of 5 km, while the yellow dotted line is the path of the magnetic foot-point of the Reimei spacecraft - the yellow X shows this point at the time of capture for each image. (d and e) Vorticity derived from the optical flow measurements; red-yellow and blue show anticlockwise and clockwise rotation around the geomagnetic field respectively.

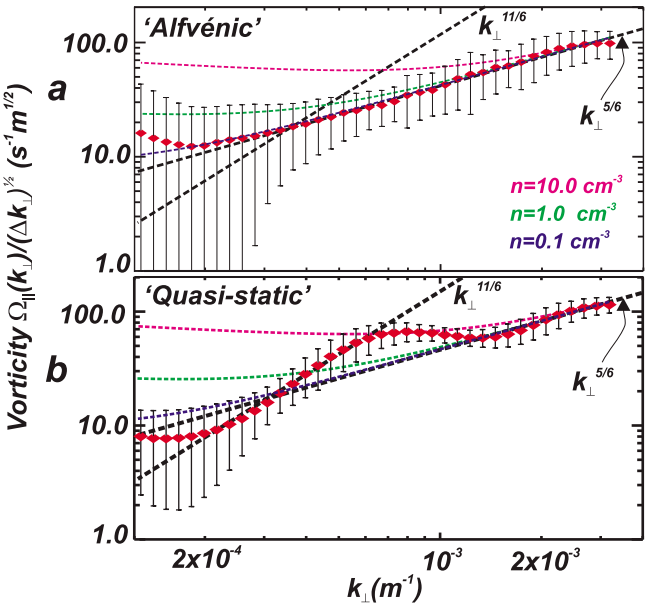

Figure 3. Vorticity spectra for the (a) Alfvénic and (b) Quasi-static aurora. Magenta, green and blue lines show expected trend in vorticity for Alfvén waves on 'infinitely conducting' geomagnetic field-lines at 4000 km altitude with the plasma densities shown in the same color; error bars represent the standard deviation in vorticity for each $k_\perp$. Black dashed lines show power-law scaling dependencies.

[6] The degree of shear and rotation in the optical forms can be quantified in terms of the geomagnetic field-aligned vorticity given by $\Omega_\parallel = \nabla \times u$. Here u is the velocity of optical features in the camera's field of view. $\Omega_\parallel$ can be derived by finite differencing of the velocity field as shown for the Alfvénic and quasi-static aurora in Figures 2d–2e. Here positive vorticity or anti-clockwise rotation about the geomagnetic field is shown in yellow-red while negative vorticity or clockwise rotation around the geomagnetic field is shown in blue-black. The distribution of vorticity shown here is indicative of the instabilities [*Wu and Seyler*, 2003; *Asamura et al.*, 2009] responsible for the evolution of the optical forms observed.

[7] The wavelet analysis facilitates a consideration of how vorticity varies as a function of perpendicular scale or wave-number ($k_\perp = 2\pi/\lambda_F$). Vorticity spectrograms ($|\Omega_\parallel(k_\perp)|/\Delta k_\perp^{1/2}$ *vs* $k_\perp$) derived using this technique for the Alfvénic and quasi-static aurora are shown in Figures 3a and 3b. These have been compiled from individual wavelet vorticity spectra recorded at each point in the images where emission intensity exceeds 50 kR and averaged over those images where the Alfvénic and quasi-static aurora remain in the field of view of the camera. The data points correspond to average values at each scale or wave-number and the error bars to 1 standard deviation in the distribution of vorticity measurements at each scale. In preparing this figure we have selected $k_{\perp x} = k_{\perp y}$ with $k_\perp^2 = k_{\perp x}^2 + k_{\perp y}^2$, however any selection of wave-numbers along the x and y axis of the images produces similar results. (We note that integrating the vorticity over all scales in either the X or Y directions provides the 1-D vorticity spectra often discussed in studies of fluid turbulence). Overall the vorticity in both the Alfvénic and quasi-static aurora increases with decreasing scale or increasing wave-number with a dependency approaching the power laws shown by the black dashed lines in Figures 3a and 3b. We note, however the vorticity in the quasi-static case increases more rapidly over the range from $k_\perp = 0.0002$–0.0007 m^{-1} (~30–8 km scales) than that of the Alfvénic aurora.

3. Discussion

[8] The scaling of the vorticity spectra can be understood if the motion of auroral forms is controlled by the electric field drift of plasmas with velocity $u = E \times B_o/B_o^2$ in geomagnetic field-aligned currents and Alfvén waves above the auroral ionosphere and the low altitude extent of the auroral acceleration region [*Hallinan,* 1981]. Here B_o is the geomagnetic field strength and E is the electric field associated with a geomagnetic field-aligned current ($J_\parallel$) given by Faraday's Law as

$$E_\perp = -b_\perp\left(\frac{\omega}{k_\parallel} - i\frac{k_\perp^2}{\mu_o k_\parallel \sigma_\parallel}\right) \quad (1)$$

where we have used $J_\parallel = \sigma_\parallel E_\parallel = ik_\perp b_\perp/\mu_o$ from Ohm's and Ampere's laws. The $\parallel$ and $\perp$ subscripts refer to geomagnetic field-aligned and perpendicular directions respectively, $\sigma_\parallel$ is the generalized conductivity, $b_\perp$ is the magnetic field due to the current and ω is the frequency. The relationship between ω, $k_\parallel$ and $k_\perp$ is given by the dispersion relation for small scale Alfvén waves in a cold plasma [*Lysak and Carlson,* 1981]. Using this dispersion relation, and the previously reported result $b_\perp^2(k_\perp)/\Delta k_\perp \approx Ck_\perp^{-7/3}$ for magnetic fluctuations in Alfvén waves above the aurora [*Chaston et al.*, 2008] we find,

$$|\Omega_\parallel(k_\perp)|\Big/\Delta k_\perp^{1/2} \approx \frac{C^{1/2}k_\perp^{-1/6}V_A\sqrt{1+k_\perp^2\lambda_e^2(1+i\nu/\omega)}}{B_o} \quad (2)$$

where C is constant, V_A is the Alfvén speed and λ_e is the electron inertial length given by the speed of light divided by the electron plasma frequency. The Ohmic conductivity ($1/[\nu\mu_o\lambda_e^2]$) along the geomagnetic field-line is incorporated through, ν, which is an effective collision frequency. We include ν here to represent the effects of finite field-line conductivity in the generation of vorticity in Alfven waves without necessarily invoking any specific process, however we note that in the case of anomalous resistivity due to velocity space instabilities ν generally exceeds ω once certain thresholds have been reached [*Lysak and Dum*, 1983]. In the limit where $k_\perp\lambda_e > 1$ or $\nu/\omega > 1$, $|\Omega_\parallel(k_\perp)|/\Delta k_\perp^{1/2}$ given by equation (2) approaches the observed $k_\perp^{5/6}$ power law shown in Figure 3 for the Alfvénic aurora but also the quasi-static aurora for $k_\perp > 0.0012$ or scales <5 km. The blue, green and magenta curves in Figure 3 show this relation for $\nu = 0$ and number densities of n = 0.1, 1.0 and 10 cm^{-3} representative of the range of particle number densities observed through the auroral acceleration region at ~4000 km altitude [*Strangeway et al.*, 1998]. Here we have mapped $k_\perp$ from the approximate base of the auroral acceleration region assumed to be at 4000 km to ~105 km - the approximate altitude of the optical emissions observed from

Reimei. Particle observations suggest that the base of the acceleration is nearly always above 2000 km [*Cattell et al.*, 1991] and below ~1 Earth radius [*Mozer and Hull*, 2001] in altitude. Assuming higher altitudes within this range will shift these curves slightly to the right and lower altitudes slightly to the left, however the power-law scaling will remain unaltered. It can be expected that reflection from the highly conducting ionosphere, not included in equation (2), will act to reduce $E_\perp$ and hence the vorticity given by equation (2) at small $k_\perp$; nonetheless, the curves for n = 0.1–1 cm^{-3} provide a good representation of the variation in the observed vorticity spectra in the Alfvénic aurora over the entire $k_\perp$ range observed.

[9] For the case where $\omega \rightarrow 0$, appropriate for the quasi-static aurora, we re-derive equation (1) taking $db_\perp/dt \rightarrow 0$ in Faraday's law and writing Ohm's law as $J_\parallel = -K\phi_\parallel$. Here $\phi_\parallel$ is the field-aligned potential and K is the field-line conductance often discussed in current-voltage studies of auroral particle acceleration [*Knight*, 1973]. Including the contribution to $E_\perp$ due to current closure through the ionosphere given by $E_{\perp i} = b_\perp/(\mu_o \Sigma_P)$ as per *Lysak* [1998] yields,

$$|\Omega_\parallel(k_\perp)| \Big/ \Delta k_\perp^{1/2} \approx C^{1/2} \frac{k_\perp^{-1/6}}{\mu_o B_o \Sigma_P}\left(1 + k_\perp^2 \lambda_{M-I}^2\right) \qquad (3)$$

where we have again made use of the result $b_\perp^2(k_\perp)/\Delta k_\perp \approx C k_\perp^{-7/3}$. Here Σ_P is the height integrated Pedersen conductivity and $\lambda_{M\text{-}I} = \sqrt{\Sigma_P/K}$ is the magnetosphere-ionosphere coupling scale length. For typically observed parameters $\lambda_{M\text{-}I}$ = 50–100 km at ionospheric altitudes. Over the range of scales covered by the Reimei spacecraft camera $k_\perp^2 \lambda_{M\text{-}I}^2 \gg 1$ so that the 2nd term in equation (3) dominates and $|\Omega_\parallel(k_\perp)|/\Delta k_\perp^{1/2}$ varies as a $\sim k_\perp^{11/6}$ power law. This power-law is plotted in Figure 3 and approximates the spectral trend shown in Figure 3b for the vorticity of the quasi-static aurora over the wave-number range $k_\perp$ = 0.0002–0.0007 m^{-1}.

4. Conclusion

[10] These results demonstrate that the complex and multi-scale motion of discrete auroral forms can be described through power-law relations governed by the physics of Alfvén waves and the effective conductivity along the geomagnetic field. Significantly the tendency towards the Alfvénic scaling in both the quasi-static and Alfvénic cases is indicative of the underlying Alfvénic nature of the electromagnetic fields supporting discrete aurora. We note that the power-law relations we observe, as in fluids generally, are indicative of cross-scale coupling and energy transport. How this transport proceeds to provide the scaling observed and drive the aurora is however unknown, and remains an outstanding task for further analyses of Reimei observations, theoretical efforts and future auroral satellite missions.

[11] **Acknowledgments.** This research was supported by STEL visiting professor program, the global COE program "Quest for Fundamental Principles in the Universe: from Particles to the Solar System and the Cosmos" of Nagoya University, NSF grant ATM-0602728 and NASA grant number NNG06GG63G. Chris Chaston thanks Robert Lysak and Ilan Roth for comments during the completion of this research.

References

Asamura, K., et al. (2003), Auroral particle instrument onboard the INDEX satellite, *Adv. Space Res.*, *32*, 375–378, doi:10.1016/S0273-1177(03)90275-4.

Asamura, K., et al. (2009), Sheared flows and small-scale Alfvén waves generation in the auroral acceleration region, *Geophys. Res. Lett.*, *36*, L05105, doi:10.1029/2008GL036803.

Cattell, C. A., S. Chari, and M. A. Temerin (1991), An S3-3 satellite study of the effects of the solar cycle on the auroral acceleration process, *J. Geophys. Res.*, *96*(A10), 17,903–17,908, doi:10.1029/91JA01824.

Chaston, C. C., L. M. Peticolas, J. W. Bonnell, C. W. Carlson, R. E. Ergun, and J. P. McFadden (2003), Width and brightness of auroral arcs driven by inertial Alfvén waves, *J. Geophys. Res.*, *108*(A2), 1091, doi:10.1029/2001JA007537.

Chaston, C. C., C. Salem, J. W. Bonnell, C. W. Carlson, R. E. Ergun, R. J. Strangeway, and J. P. McFadden (2008), The turbulent Alfvénic aurora, *Phys. Rev. Lett.*, *100*, 175003, doi:10.1103/PhysRevLett.100.175003.

Ebihara, Y., Y.-M. Tanaka, S. Takasaki, A. T. Weatherwax, and M. Taguchi (2007), Quasi-stationary auroral patches observed at the South Pole Station, *J. Geophys. Res.*, *112*, A01201, doi:10.1029/2006JA012087.

Ergun, R. E., et al. (1998), FAST satellite observations of electric field structures in the auroral zone, *Geophys. Res. Lett.*, *25*, 2025–2028, doi:10.1029/98GL00635.

Frank, L., and K. Ackerson (1972), Local-time survey of plasma at low altitudes over the auroral zones, *J. Geophys. Res.*, *77*(22), 4116–4127, doi:10.1029/JA077i022p04116.

Hallinan, T. J. (1981), The distribution of vorticity in auroral arcs, in *Physics of Auroral Arc Formation*, *Geophys. Monogr. Ser.*, vol. 25, edited by S.-I. Akasofu and J. R. Kan, pp. 42–49, AGU, Washington, D. C.

Hallinan, T. J., et al. (2001), Relation between optical emissions, particles, electric fields, and Alfvén waves in a multiple rayed arc, *J. Geophys. Res.*, *106*, 15,445–15,454, doi:10.1029/2000JA000321.

Kletzing, C. A. (1994), Electron acceleration by kinetic Alfvén waves, *J. Geophys. Res.*, *99*, 11,095–11,103.

Knight, S. (1973), Parallel electric fields, *Planet. Space Sci.*, *21*, 741–750, doi:10.1016/0032-0633(73)90093-7.

Lysak, R. L. (1998), The relationship between electrostatic shocks and kinetic Alfvén waves, *Geophys. Res. Lett.*, *25*, 2089–2092, doi:10.1029/98GL00065.

Lysak, R. L., and C. W. Carlson (1981), Effect of micro-turbulence on magnetosphere-ionosphere coupling, *Geophys. Res. Lett.*, *8*, 269–272, doi:10.1029/GL008i003p00269.

Lysak, R. L., and C. T. Dum (1983), Dynamics of magnetosphere-ionosphere coupling including turbulent transport, *J. Geophys. Res.*, *88*, 365, doi:10.1029/JA088iA01p00365.

Lysak, R. L., and W. Lotko (1996), On the kinetic dispersion relation for shear Alfvén waves, *J. Geophys. Res.*, *101*, 5085, doi:10.1029/95JA03712.

Mozer, F., and A. Hull (2001), Origin and geometry of upward parallel electric fields in the auroral acceleration region, *J. Geophys. Res.*, *106*, 5763–5778, doi:10.1029/2000JA900117.

Mozer, F. S., C. W. Carlson, M. K. Hudson, R. B. Torbert, B. Parady, J. Yatteau, and M. C. Kelley (1977), Observations of paired electrostatic shocks in the polar magnetosphere, *Phys. Rev. Lett.*, *38*, 292, doi:10.1103/PhysRevLett.38.292.

Obuchi, Y., et al. (2008), Initial observations of auroras by the multi-spectral auroral camera on board the Reimei satellite, *Earth Planets Space*, *60*, 827–835.

Sakanoi, T., et al. (2003), Development of the multi-spectral auroral camera onboard the INDEX satellite, *Adv. Space Res.*, *32*, 379–384, doi:10.1016/S0273-1177(03)90276-6.

Stasiewicz, K., et al. (2000), Small scale Alfvénic structure in the aurora, *Space Sci. Rev.*, *92*, 423–533, doi:10.1023/A:1005207202143.

Stenbaek-Nielsen, H. C., T. J. Hallinan, D. L. Osborne, J. Kimball, C. C. Chaston, J. P. McFadden, G. Delory, M. Temerin, and C. W. Carlson (1998), Aircraft observations conjugate to FAST: Auroral Arc thicknesses, *Geophys. Res. Lett.*, *25*, 2073–2076, doi:10.1029/98GL01058.

Strangeway, R. J., et al. (1998), FAST observations of VLF waves in the auroral zone: Evidence of very low plasma densities, *Geophys. Res. Lett.*, *25*, 2065–2068, doi:10.1029/98GL00664.

Torrence, C., and G. P. Compo (1998), A practical guide to wavelet analysis, *Bull. Am. Meteorol. Soc.*, *79*, 61–78, doi:10.1175/1520-0477(1998)079<0061:APGTWA>2.0.CO;2.

Wu, K., and C. E. Seyler (2003), Instability of inertial Alfvén waves in transverse sheared flow, *J. Geophys. Res.*, *108*(A6), 1236, doi:10.1029/2002JA009631.

K. Asamura, Institute of Space and Astronautical Science, Japan Aerospace Exploration Agency, Kanagawa 229-8510, Japan.

C. C. Chaston, Space Sciences Laboratory, University of California, Berkeley, CA 94720, USA. (ccc@ssl.berkeley.edu)

M. Hirahara, Department of Earth and Planetary Science, Graduate School of Science, University of Tokyo, Tokyo 113-0033, Japan.

T. Sakanoi, Graduate School of Science, Planetary Plasma and Atmospheric Research Centre, University of Tohoku, Sendai 980-8578, Japan.

K. Seki, Solar Terrestrial Environment Laboratory, University of Nagoya, Nagoya 464-8601, Japan.